

# System and Energy Dependence of Strangeness Production with STAR

Sevil Salur<sup>a</sup> (for the STAR<sup>†</sup> Collaboration)

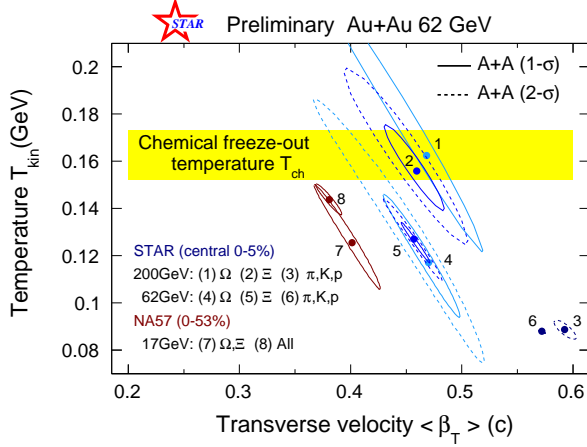
<sup>a</sup> Physics Department, Yale University, P.O. Box 208120, New Haven, CT, 06520, USA

The yields and spectra of strange hadrons have each been measured by STAR as a function of centrality in  $\sqrt{s_{\text{NN}}} = 200$  GeV AuAu collisions. By comparing to pp and dAu at  $\sqrt{s_{\text{NN}}} = 200$  GeV and in AuAu at  $\sqrt{s_{\text{NN}}} = 62$  GeV the dependence on system size and energy is studied. Strange resonances, such as  $\Sigma(1385)$  and  $\Lambda(1520)$ , are used to examine the dynamical evolution between production and freeze-out for these systems. Particle production is investigated by comparison to thermal models, which assume a scaling of the yield with  $N_{\text{part}}$ . Our hyperon measurements in AuAu indicate that  $N_{\text{bin}}$  may be a more appropriate scale for the strangeness correlation volume. Thus canonical suppression can not be simply parameterized with the geometrical overlap volume but will depend on the individual quark content of each particle. This theory is tested by comparing the data from different collision systems and centralities.

## 1. Introduction

RHIC has been run in various configurations of pp, CuCu, dAu, and AuAu at energies ranging from  $\sqrt{s_{\text{NN}}} = 19$  to 200 GeV. These rich data sets, together with STAR's large acceptance, provide the best opportunity to study strange particles in dense systems. As the strange quark is the next-lightest after the up and down quarks and does not exist in the initial colliding system, investigation of its production and dynamics may reveal some of the properties of strongly interacting matter at high densities. A hydrodynamically inspired Blast-Wave parametrization with fit parameters kinetic temperature  $T_{\text{Kin}}$  at freeze-out, mean transverse flow velocity  $\langle\beta_{\text{T}}\rangle$ , and a normalization factor, is used to fit the data [1, 2]. The one and two  $\sigma$  fit contours of the  $T_{\text{Kin}}$  and  $\langle\beta_{\text{T}}\rangle$  parameters from a Blast-Wave fit to  $\pi$ , K, p and strange particles are presented in Figure 1 for  $\sqrt{s_{\text{NN}}} = 17.3, 62.4$  and 200 GeV collision energies. The variation of the fit parameters indicates that the spectral shapes are different for the different particles. The  $T_{\text{Kin}}$  parameter is higher (hotter source) and  $\langle\beta_{\text{T}}\rangle$  is lower (less flow) for baryons with higher strange quark content at the same collision energy. While the  $\langle\beta_{\text{T}}\rangle$  remains almost unchanged, the  $T_{\text{Kin}}$  parameter for the multi-strange baryons is lower at  $\sqrt{s_{\text{NN}}} = 62$  GeV than at 200 GeV. This behavior is different for  $\pi$ , K, and p where the  $\langle\beta_{\text{T}}\rangle$  is larger at 200 GeV though  $T_{\text{Kin}}$  is the same. For SPS collisions at  $\sqrt{s_{\text{NN}}} = 17.3$  GeV, the parameters follow similar trends

<sup>†</sup>For the full list of STAR authors and acknowledgments, see appendix 'Collaborations' of this volume.



as at RHIC. The differences between the fit parameters imply variations in dynamical properties of the collision energies, while in terms of chemical properties the results from  $\sqrt{s_{NN}} = 62.4$  and 200 GeV collisions are equivalent [4].

Figure 1.  $1\sigma$  and  $2\sigma$  error contours representing Blast-Wave fits to particles from the most central AuAu collisions at RHIC and PbPb collisions at SPS.

## 2. System Size Dependence Of Strange Particles

The energy dependence of  $\Lambda$  and  $\bar{\Lambda}$  yields at mid-rapidity from AuAu collisions at RHIC and PbPb collisions at SPS as a function of  $\sqrt{s_{NN}}$  is presented in Figure 2-a. From SPS to RHIC energies, strange baryon production is approximately constant at mid-rapidity, whereas the  $\bar{\Lambda}$  rises steeply, reaching 80% of the  $\Lambda$  yield at RHIC top energies. The other hyperons -  $\Xi$ ,  $\Omega$  and  $\Sigma(1385)$ - follow similar trends. This implies that at low energies, strange baryon production is dominated by transport from the colliding system but at RHIC it is dominated by pair production. Figure 2-b shows the  $\bar{\Lambda}/\Lambda$  ratios with respect to the number of participants for the collisions at SPS and RHIC. Within errors, the  $\bar{\Lambda}/\Lambda$  ratios are nearly independent of the system size in AuAu collisions of the same energy at RHIC. There is a decrease in the  $\bar{\Lambda}/\Lambda$  ratio moving from pp to dAu to AuAu.

Figure 2-c shows the ratio of strange resonances to their corresponding stable particles normalized to their values in pp. While the  $\Sigma(1385)/\Lambda$  ratio is independent of system size at 200 GeV and is consistent with lower energy pp values, other ratios such as  $K^*/K$  and  $\Lambda(1520)/\Lambda$  show a slight suppression in AuAu collisions, independent of centrality. Due to their short lifetimes, the re-scattering of resonance decay products between chemical and thermal freeze-out is expected to cause a signal loss. While the observed suppression of  $K^*/K$  and  $\Lambda(1520)/\Lambda$  corroborates the re-scattering picture, the lack of suppression of the  $\Sigma(1385)/\Lambda$  ratio implies a recovery mechanism such as regeneration (e.g.  $\Lambda + \pi \rightarrow \Sigma(1385)$ ). The total interaction cross sections with  $\pi$  increases from K to p to

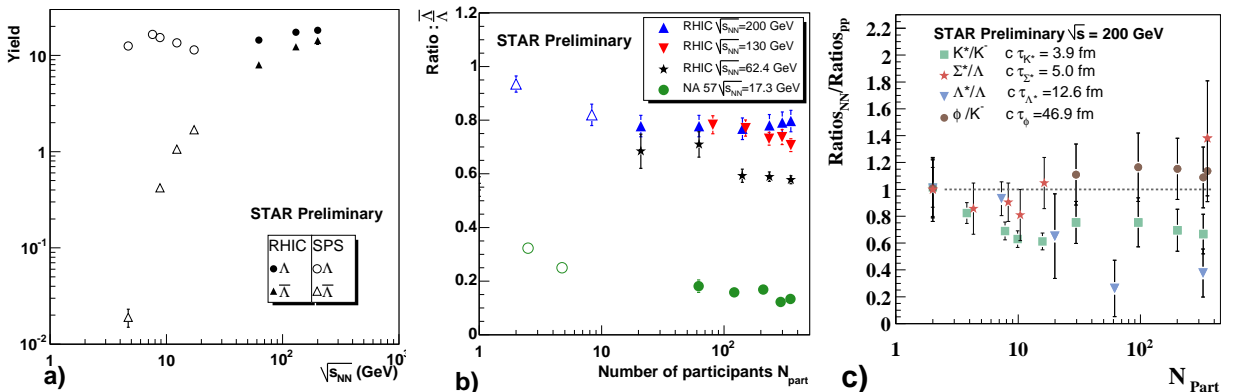
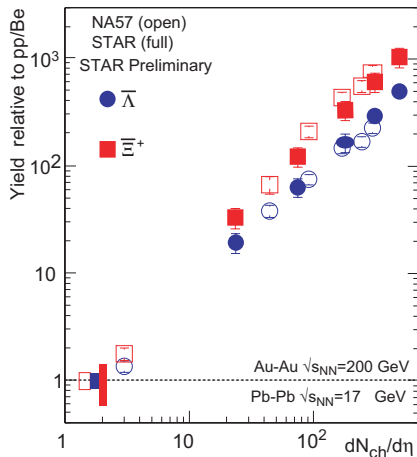


Figure 2. (a) The  $\sqrt{s_{NN}}$  dependence of  $\Lambda$  and  $\bar{\Lambda}$  yields. (b) The dependence of  $\bar{\Lambda}/\Lambda$  on number of participants for various collision energies. (c) Resonance to stable particle ratios normalized to pp for pp, dAu and AuAu collisions at  $\sqrt{s_{NN}} = 200$  GeV [5, 6, 7].

$\pi$  respectively [ 8]. This implies that re-scattering of  $K^*$  decaying into  $\pi$  and  $K$  in the medium should be higher than that of  $\Lambda(1520)$  decaying into  $K$  and  $p$ . The shorter lifetime of  $K^*$  enhances the re-scattering probability. In this scenario, assuming that the lifetime between chemical and thermal freeze-out is non-zero, the regeneration cross-section for  $K^*$  must be larger than that of  $\Lambda(1520)$  due to the smaller suppression of the  $K^*$  ratios.

HBT radii show a linear dependence on  $dN_{\text{ch}}^{1/3}/d\eta$ , a term related to the final state geometry through the density at freeze-out [ 9]. If entropy drives the strangeness yield, results from different collision energies at the SPS and RHIC should exhibit universal scaling with entropy. Figure 3 presents the yields of  $\bar{\Lambda}$ ,  $\bar{\Xi}$  in AuAu collisions at RHIC, normalized to yields in pp and in PbPb collisions at the SPS, normalized to yields in pBe, as a function of  $dN_{\text{ch}}/d\eta$  ( $\sim$  entropy). Strange yields in heavy ion collisions, when compared to lighter systems, seem to universally scale with  $dN_{\text{ch}}/d\eta$  for SPS and RHIC energies. It is also predicted that the greater the number of strange quarks in the particle, the greater the effect of phase space suppression when modeled with respect to the number of participants,  $N_{\text{part}}$  [ 10]. Even though the expected ordering of the suppression is observed at RHIC, the  $\bar{\Lambda}$  and  $\bar{\Xi}$  measurements normalized to their pp values do not



flatten at larger  $N_{\text{part}}$ , in variance to predictions [ 11]. This might be because strange particles scale differently from non-strange. Particles with only  $u$  and  $d$  quarks are already observed to scale with  $N_{\text{part}}$  while strange quarks appear to scale better with  $N_{\text{bin}}$ .  $N_{\text{part}}$  and  $N_{\text{bin}}$  can be combined to form a correlation volume for strange particles which depends on the quark content. This combined scaling seems to represent the strange particles better than  $N_{\text{part}}$  alone.

Figure 3. The dependence on  $dN_{\text{ch}}/d\eta$  of the  $\bar{\Lambda}$  and  $\bar{\Xi}$  yields in AuAu relative to pp at RHIC and in PbPb relative to pBe at SPS energies.

Nuclear modification factors for strange particles in AuAu collisions are presented in Figure 4. At higher  $p_{\text{T}}$ , the ratios exhibit a suppression from binary scaling, attributed to fast moving partons losing energy as they traverse a dense medium. The  $R_{\text{CP}}$  from  $\sqrt{s_{\text{NN}}} = 62.4$  GeV shows less suppression than that at  $\sqrt{s_{\text{NN}}} = 200$  GeV; however, the clear differences between baryons and mesons still exists [ 12]. This is believed to be due to hadron production through quark coalescence at intermediate  $p_{\text{T}}$  [ 13]. For baryons and mesons, the suppression sets in at a different  $p_{\text{T}}$ . Motivated by the coalescence picture, Figure 4-b shows the  $R_{\text{CP}}$  ratio vs  $p_{\text{T}}/n$  for  $\sqrt{s_{\text{NN}}} = 62.4$  GeV, where  $n$  is the number of valence quarks. Thus  $p_{\text{T}}/n$  is the  $p_{\text{T}}$  of a quark. The baryon and meson sets in at the same quark  $p_{\text{T}}$ , in agreement with the coalescence picture. This is also observed for  $\sqrt{s_{\text{NN}}} = 200$  GeV collisions. The measurement of  $R_{\text{AA}}$  with respect to  $p_{\text{T}}$  is shown in Figure 4-c. While the  $R_{\text{AA}}$  for mesons ( $h^+ + h^-$ ,  $K_{\text{S}}^0$ ,  $\phi$ ) is similar to their  $R_{\text{CP}}$  values,  $R_{\text{AA}}$  of strange baryons shows significant differences (i.e. no suppression). Instead, there is an enhancement and ordering with strangeness content: the higher the strangeness content, the higher the  $R_{\text{AA}}$  measurement in the intermediate  $p_{\text{T}}$  region. The difference between yields in pp and peripheral AuAu may be explained by phase space (canonical) suppression in the pp data-set although this is usually attributed to low  $p_{\text{T}}$  particles [ 14].

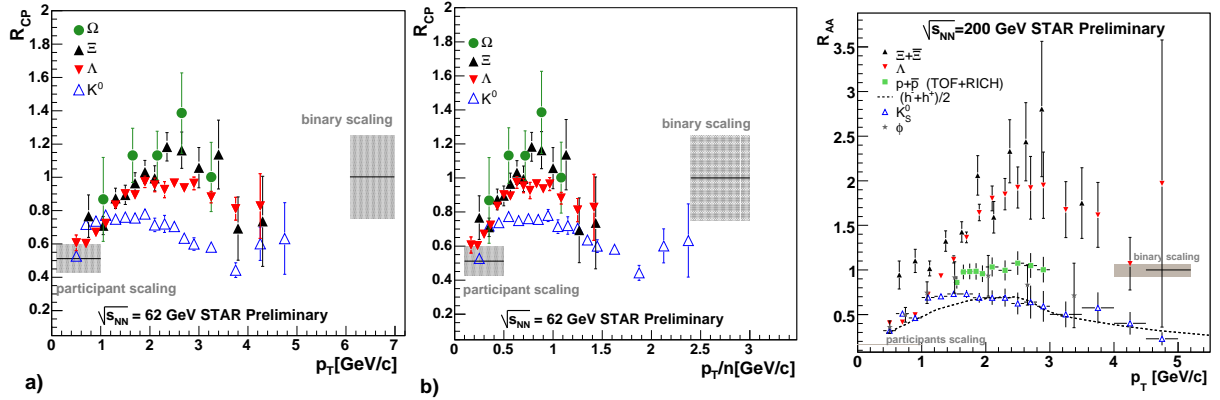


Figure 4. (a)  $R_{CP}$  vs  $p_T$  at  $\sqrt{s_{NN}} = 62.4$  GeV. (b)  $R_{CP}$  vs  $p_T/n$  at  $\sqrt{s_{NN}} = 62.4$  GeV. (c)  $R_{AA}$  at  $\sqrt{s_{NN}} = 200$  GeV with respect to  $p_T$ .  $R_{CP}$  is calculated from 0-5% and 40-60% central AuAu collisions and  $R_{AA}$  is from 0-5% central AuAu and min-bias pp collisions.

### 3. Conclusions

Dynamical properties of strange particles can be investigated by Blast-Wave fits. The  $\langle\beta_T\rangle$  increases with collision energy, implying a higher flow and the freeze-out temperatures of multi-strange baryons are larger than those of light mesons, suggesting an earlier freeze-out (e.g.  $T(\Xi) > T(\pi)$ ). Strange anti-baryon and baryon production are approximately equal at top RHIC energies. There is a slight decrease in the  $\bar{\Lambda}/\Lambda$  ratio from pp to dAu to AuAu, indicating that baryon number transport is almost independent of system size. Resonance yields require both re-scattering and regeneration mechanisms for  $\Delta t > 0$  between chemical and thermal freeze-out to describe the suppression in some of their yields. Strange quarks appear to scale better with the number of hard processes ( $N_{bin}$ ), while light quarks scale with  $N_{part}$  and strange particle yields seem to universally scale with  $dN_{ch}/d\eta$  for SPS and RHIC. The meson/baryon separation of the nuclear modification factors also exists in  $\sqrt{s_{NN}} = 62$  GeV collisions which can be explained in a coalescence picture. The  $R_{AA}$  of strange baryons behave differently from their  $R_{CP}$ . Canonical suppression in pp might explain the observed difference, though it is a surprise that this effect extends to intermediate  $p_T$ .

### REFERENCES

1. P.F. Kolb and U.Heinz, nucl-th/0305084.
2. J. Speltz (for the STAR Collaboration), QM 2005 Poster; L. Molnar, nucl-ex/0507027.
3. F. Antinori et al. (NA57 Collaboration) J. Phys. G 30 (2004) 823
4. O. Barannikova (for the STAR Collaboration) J. Phys. G 31, (2005) S93.
5. D. Mishra (for the STAR Collaboration), QM 2005 Poster Presentation.
6. S. Salur (for the STAR Collaboration), Eur. Phys. J. C 40, (2005) s3.9-s3.13.
7. C. Markert (for the STAR Collaboration), QM 2005 Poster Presentation.
8. S. Eidelman et al., Phys. Lett. B 592, 1 (2004).
9. M. Lisa, S. Pratt, R. Soltz, and U. Wiedemann, (2005) nucl-ex/0505014.
10. A. Tounsi, A. Mischke and K. Redlich, Nucl. Phys. A 715, 565 (2003).
11. H. Caines (for the STAR Collaboration), J. Phys. G 31, (2005) S101-S118.
12. J. Adams et al. (STAR Collaboration) Phys. Rev. Lett. 92 (2004) 052302.
13. M. Lamont (for the STAR Collaboration), J. Phys. G 30, (2004) S963-S967.
14. K. Redlich and A. Tounsi, Eur. Phys. J. C 24, 589-594 (2002).